

Seed-layer effect on the microstructure and magnetic properties of Co/Pd multilayers

A. G. Roy and D. E. Laughlin

Data Storage Systems Center, Carnegie Mellon University, Pittsburgh, Pennsylvania 15213-3890

T. J. Klemmer,^{a)} K. Howard, S. Khizroev, and D. Litvinov

Seagate Research, Pittsburgh, Pennsylvania 15203-2116

We have investigated Co/Pd multilayers deposited on either Ta or indium tin oxide (ITO) seed layers as a potential perpendicular recording media. We have examined the microstructural evolution of the films deposited on the two different types of seed layers and related it to the magnetic properties of the films. Ta underlayer produces a strong $\langle 111 \rangle$ fiber texture in the multilayer while ITO produces randomly oriented grains. Transmission electron microscopy reveals a microstructure of columnar grains separated by less dense material at the boundaries for the multilayers with an ITO underlayer. However, the less dense material is absent when using a Ta underlayer. The films exhibited strong perpendicular anisotropy and a higher coercivity of ~ 6800 Oe and squareness of ~ 0.99 are obtained for the films deposited on an ITO seed layer. The differences in the value of coercivity and squareness in the films can be correlated with the differences in the evolution of microstructures for different seed layers. © 2001 American Institute of Physics. [DOI: 10.1063/1.1360685]

I. INTRODUCTION

Perpendicular magnetic recording is being considered as a candidate for achieving extremely high density recording with high thermal stability.¹⁻³ Traditional perpendicular films of hexagonal Co alloys usually have low squareness without correction for demagnetization and large dc-erase noise since the perpendicular anisotropy is insufficient to overcome the high demagnetization field. Co/Pt and Co/Pd superlattices have been extensively studied for magneto-optical recording.^{4,5} Their high interface-induced perpendicular anisotropy, high coercivity, and high squareness also make them promising candidates for perpendicular recording. One of the challenges of these materials is the control of the magnetization reversal process that strongly depends on the film microstructure. Control of the magnetization reversal mechanism in Co/Pd multilayers by underlayer processing has been reported.⁶ Here we describe the effect of two different seed layers on structure evolution and magnetic properties of Co/Pd superlattices. Ta was chosen for the study because of the enhancements often observed in magnetic properties when Ta is used as a seed layer for other applications. Amorphous indium tin oxide (ITO) was chosen for this study because of the recent reports of coercivity enhancement in Co/Pt and Co/Pd superlattices when using ultrathin ITO seed layers.^{7,8} Although ITO is known as a ceramic material of somewhat novel electronic properties, these recent reports point to ITO as being a viable seed layer for future perpendicular media.

II. EXPERIMENT

Two types of Co/Pd superlattices were deposited by magnetron sputtering at ambient temperature on Al substrates coated with NiP.

Type I: Ta(15 nm)\{Co(0.3 nm)\Pd(1 nm)\}₂₀.

Type II: Ta(5 nm)\ITO(2 nm)\{Co(0.3 nm)\Pd(1 nm)\} × 20.

The base pressure in the deposition system was 10^{-7} Torr. Krypton at 30 mTorr was used as a sputtering gas for Co and Pd. The deposition rates for Co and Pd were 0.15 and 1.0 nm/s, respectively. Ta and ITO seed layers were sputtered in 15 mTorr of Ar with deposition rates of 2.5 and 1.7 nm/s, respectively.

A polar Kerr magnetometer was used to measure the Kerr hysteresis loops. The structure of the films was determined by using a Philips X-Pert Pro x-ray diffractometer and transmission electron microscopy (TEM). The x-ray optics utilized in high angle x-ray scans and rocking curves involved an x-ray mirror while the in-plane measurements utilized an x-ray lens. The compositional distribution of the samples was studied by electron energy loss spectroscopy (EELS).

III. RESULTS AND DISCUSSION

Figure 1 shows the perpendicular Kerr loops for Co/Pd multilayers deposited on Ta and ITO. The shape of the loops and the coercivities are found to be quite different from each other. From the coercive squareness and the slope of the hysteresis loops, it can be observed that the Ta underlayer produces a magnetic multilayer that is more exchange coupled than the ITO underlayer. The coercivity for the film with the ITO underlayer is about 6800 Oe, which is about two times larger than the film with the Ta underlayer. The differences in the magnetic properties between the two types of films are due to the underlayer effect on structure evolution.

The microstructural evolution of Co/Pd multilayers as a function of the type of seed layer has been observed by both plan-view and cross-sectional TEM. The plan-view TEM

^{a)}Electronic mail: timothy.j.klemmer@seagate.com

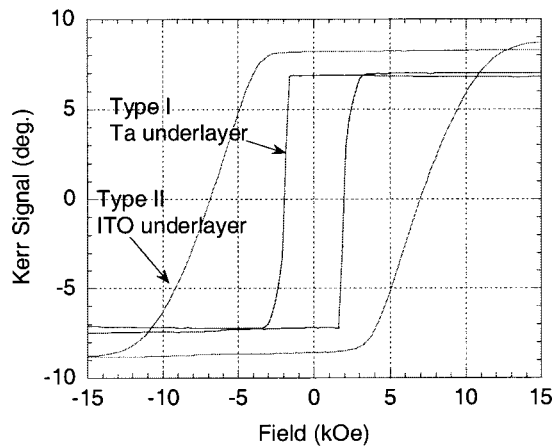


FIG. 1. Kerr loops for type-I and type-II films.

bright field images of the Co/Pd layers with different seed layers are shown in Fig. 2. The grain sizes of the Co/Pd layers with and without ITO can be easily determined from the dark field images. The average grain size was typically around 6 nm for the multilayers with the Ta seed and the ITO produced a slightly larger grain size. The samples with ITO seed layers show granular structures [Fig. 2(b)]. The “columns” are distinctly separated with a boundary, which looks like a channel network. The average column diameter is about 20 nm. From the respective dark field images it was determined that the columns consisted of several individual smaller grains for the sample with ITO seed layers [Fig. 2(d)].

The texture was measured by rocking curve x-ray diffraction (XRD) profiles. Figure 3 shows the distribution of

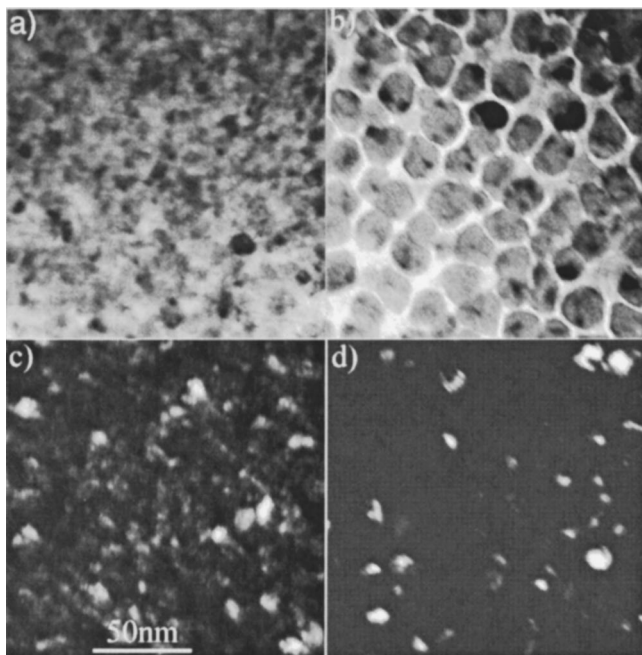


FIG. 2. Typical plan-view TEM images of CoPd layers: (a) and (b) are the bright field images for type-I and type-II film, respectively; (c) and (d) are their corresponding dark field images taken from the combined CoPd (111) and (200) rings.

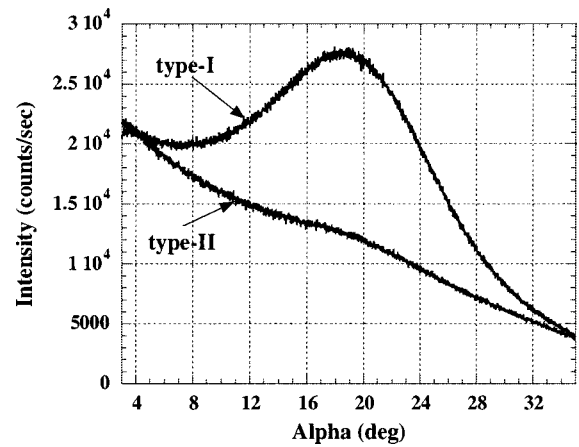


FIG. 3. CoPd(111) rocking curves for type-I and type-II films.

(111) poles in the vicinity of the sample normal for type-I and type-II films. The increasing background with decreasing alpha in the plots results from a larger excited volume of the film at low grazing incidence angles. The rocking curves also suggest that the Ta underlayer produces a stronger $\langle 111 \rangle$ fiber texture in the multilayer while ITO produces randomly oriented grains. The $\Delta\theta_{50}$ for type-I film is $\sim 12^\circ$. Evidently the ITO intermediate seed layer destroys the texture of the films. The observation of a randomly oriented Co/Pd multilayer using the ITO seed layer is contrary to the earlier reported result.⁸ However, it should not be too surprising that a high coercivity is not consistent with having strong $\langle 111 \rangle$ fiber texture. The fundamental magnetic anisotropy and therefore coercivity should have a weak dependence on crystallographic texture (contrary to conventional hcp Co media) since the multilayers are predominantly controlled by interfacial anisotropy. Additionally it is known from epitaxially grown Co/Pd multilayers that the interface anisotropy for this system has little dependence on the crystallographic orientation.⁹

Figure 4 shows in-plane XRD¹⁰ profiles for Co/Pd superlattices with and without ITO seed layers. This type of XRD scan probes (hkl) planes with normals perpendicular to the sample normal. At the low angles a peak for β -Ta is observed. Both multilayers show the peaks of fcc (111), (200), and (220) with the calculated lattice parameter (a_0)

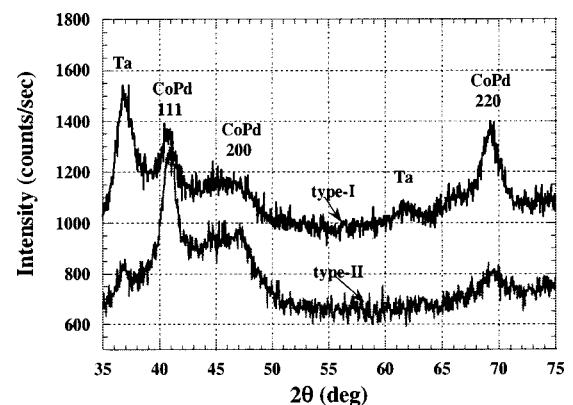


FIG. 4. In-plane XRD profiles of type-I and type-II films.

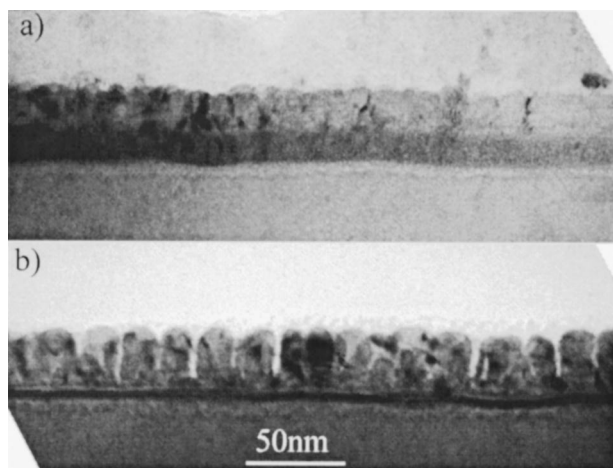


FIG. 5. Cross-sectional TEM images: (a) type-I and (b) type-II films.

~ 0.381 nm) being in between that for fcc Co ($a_0 = 0.354$ nm) and fcc Pd ($a_0 = 0.389$ nm). However, since the actual Co layer is thinner than three atomic (111) planes it is difficult to distinguish between the hcp ($AB\cdots$) and fcc ($ABC\cdots$) stacking. The film with the Ta seed layer shows a relatively sharp intense (220) peak and weak (111) peak. This is consistent with Ta promoting a better $\langle 111 \rangle$ fiber texture parallel to the sample normal. The broad hump in the vicinity of the (111) and (200) is from the amorphous NiP layer.

Cross-sectional TEM observation of the sample with the Ta seed layer showed a continuous film [Fig. 5(a)]. On the other hand, the cross-sectional image for the samples with an ITO seed layer showed the truly “columnar” nature of the multilayer growth [Fig. 5(b)]. The column diameter for type-II film is about 20 nm. The columns are well-separated, consistent with plan-view images, except possibly near the bottom of the structure. The upper surface of the multilayer with the ITO underlayer was rougher as compared to that of the sample without the ITO layer.

The film with the ITO shows grains and columns that are well-separated from each other and is the most striking difference in a comparison with the Ta underlayer (Figs. 2 and 5). It is reasonable that this typical microstructure, i.e., the separation of the columns in the film with the ITO underlayer, is responsible for increasing the coercivity and decreasing the exchange coupling. The compositional distribution was checked by electron-energy-loss images. Figure 6 shows the compositional distribution of the type-II sample which has the ITO intermediate seed layer. Figure 6(a) is a zero electron-energy-loss image. Figures 6(b) and 6(c) are the Co and Pd mapping of the same image. The Co and Pd mapping shows that the amount of both Co and Pd at the boundary is lower than within the columns. This suggests that the columns in the sample with the ITO are separated by a boundary of less dense material. Presumably these boundaries are weaker magnetically which accounts for the degradation of the magnetic exchange coupling.

It is believed that the wetting nature of the underlayers and the high sputtering pressures are the reasons for the dras-

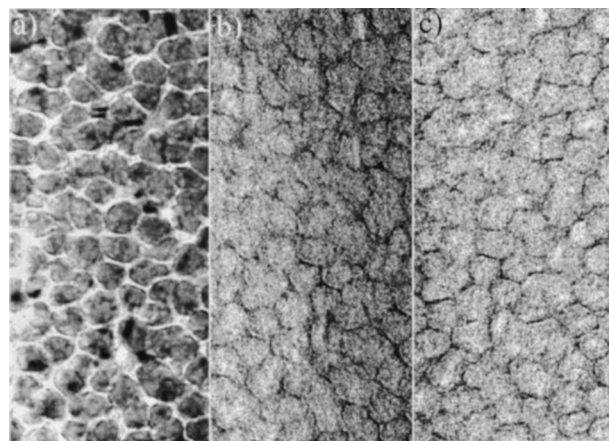


FIG. 6. Typical EELS of type-II film: (a) is zero energy loss spectrum, (b) and (c) are the Co and Pd mapping of (a), respectively.

tic difference in the microstructure of the multilayer films. Since Ta is metallic and ITO nonmetallic, the Co/Pd film can better wet the surface of Ta producing smoother initial layers. However, the ITO seed results in rougher Co/Pd initial layers. It is known that high sputtering pressures cause the phenomenon of shadowing due to the randomization of the direction of impingement of arriving atoms. For rough initial layers shadowing will be more drastic and result in rougher subsequent layers and eventually columns of more dense material separated by the less dense material.

IV. CONCLUSION

Co/Pd superlattices have been deposited by magnetron sputtering on Ta and ITO seed layers for perpendicular recording. The ITO underlayer is found to be beneficial to the fundamental perpendicular magnetic media properties and produces a magnetic multilayer that is less exchanged coupled when compared to the Ta underlayer. We have correlated the microstructure and magnetic properties. TEM microscopy and electron-energy-loss spectroscopy (EELS) reveal a microstructure of columns separated by less dense material at the boundaries for the multilayers with an ITO underlayer. These boundaries act to exchange decouple the columns from each other. However, the less dense material is absent when using a Ta underlayer.

¹K. Ouchi, TMRC'99.

²B. M. Lairson, J. Perez, and C. Baldwin, IEEE Trans. Magn. **30**, 4014 (1994).

³K. Ho, B. M. Lairson, Y. K. Kim, G. I. Noyes, and S. Sun, IEEE Trans. Magn. **34**, 1854 (1998).

⁴W. B. Zeper, H. W. V. Kesteren, B. A. J. Jacobs, J. H. M. Spruit, and P. F. Garcia, J. Appl. Phys. **70**, 2264 (1991).

⁵T. Suzuki, H. Notarys, D. C. Dobbertin, C. Lin, D. Weller, D. C. Miller, and G. Gorman, IEEE Trans. Magn. **28**, 2754 (1992).

⁶S. N. Piramanayagam, M. Matsumoto, A. Morisako, S. Takei, and D. Kadowaki, IEEE Trans. Magn. **33**, 3247 (1997).

⁷T. K. Hatwar and C. F. Brucker, IEEE Trans. Magn. **31**, 3256 (1995).

⁸W. Peng, R. H. Victora, J. H. Judy, K. Gao, and J. M. Sivertsen, J. Appl. Phys. **87**, 6358 (2000).

⁹M. T. Johnson, P. J. H. Bloemen, F. J. A. den Broedert, and J. J. de Vries, Rep. Prog. Phys. **59**, 1409 (1996).

¹⁰S. Li, C. Potter, D. Palmer, D. D. Eberl, T. Klemmer, J. Spear, C. Reiss, and D. Brown (these proceedings).